Microseismic Source Inversion in Anisotropic Media

Scott Leaney*

Schlumberger WesternGeco, Houston, USA

leaney@slb.com

and

Chris Chapman

Schlumberger Cambridge Research, Cambridge, UK

Tadeusz Ulrych

University of British Columbia

Summary

Microseismic source mechanisms are of interest in hydraulic stimulation because of what they may reveal about the induced or enhanced fracture network. Since rocks are in general anisotropic, particularly shales, it is of interest to consider what impact anisotropy may have on microseismic sources and their inversion. The strongest and most prevalent type of anisotropy in sedimentary rocks is transverse isotropy with a symmetry axis normal to bedding or vertical (so-called VTI). While the theory used is valid for general anisotropy we consider presently only layered VTI models.

An earthquake may be represented as a displacement discontinuity across a plane, composed of a double couple (DC) or shear slip component and an opening (or closing) component. While this type of source description seems physically intuitive for microseismic sources generated by hydraulic stimulation, it is an incomplete description of a moment tensor; the addition of a pure explosion (or implosion) component is necessary. We are calling such a three part Explosion + Opening + Slip source an "EOS" source, from which the moment tensor can be constructed. A theory has been developed to decompose any moment tensor M into an EOS source, given the anisotropic medium local to the source (Chapman and Leaney, 2011).

Previously we looked at the influence of anisotropy at the event location on the source including radiation patterns (Leaney and Chapman, 2010) for different EOS sources and found that if displacement was not in the symmetry axis of the medium, then the presence of anisotropy would produce false non-DC components and the focal plane solutions would be significantly distorted from their true orientations. In the present work we recover such an EOS source using three steps: 1. a ray-based, frequency domain, linear inversion for the moment tensor and source function; 2. a nonlinear inversion to obtain the scalar moment from the estimated source function; 3. a new decomposition of the moment tensor given the anisotropic medium local to the source (Chapman and Leaney, 2011). We illustrate this new anisotropic moment tensor inversion and decomposition on synthetic data. Interpretation strategies that these new analysis tools make possible are being explored.

Method

Consider vector displacement data at frequency ω, $\mathbf{u}(\omega, \mathbf{x}_j, \mathbf{x}_s)$, at receiver location $\mathbf{x}_j$ for a source at location $\mathbf{x}_s$ in terms of the moment rate tensor $\mathbf{M}(\omega)$. In the geometrical ray approximation (Chapman, 2004):

$$\mathbf{u}(\omega, \mathbf{x}_s, \mathbf{x}_j) = \left(\sum_{k}^{rays} \hat{\mathbf{g}}_k(\mathbf{x}_s, \mathbf{x}_j) G_k(\omega, \mathbf{x}_s, \mathbf{x}_j) E_k \right) : \mathbf{M}(\omega) \tag{1}$$

where it is assumed that all elements of the moment rate tensor $\mathbf{M}(\omega)$ have the same frequency (or time) dependence so that $\mathbf{M}(\omega) = \sqrt{2}M_0(\omega)\hat{\mathbf{M}}$, where $\hat{\mathbf{M}}$ is the normalized moment tensor and $M_0(\omega)$ is the scalar moment rate source-time function. In (1) G_k is the scalar ray propagation term corresponding to the third-order stress-glut Green tensor for a given ray type, k, $\hat{\mathbf{g}}_k$ is the normalized ray polarization vector at the receiver, and $E_k = (\hat{\mathbf{p}}\hat{\mathbf{g}}^T + \hat{\mathbf{g}}\hat{\mathbf{p}}^T)/2$ is the second-order ray strain tensor at the source with $\hat{\mathbf{p}}$ the normalized phase slowness vector and $\hat{\mathbf{g}}$ the polarization vector. The symbol $:$ signifies the scalar product between tensors. All terms inside the brackets come from the ray tracer, and while (1) is valid for general anisotropy, presently we consider only the VTI case. Anisotropy impacts not only the source radiation pattern ($E_k : \mathbf{M}$) and receiver polarization but also the propagation terms hidden inside G – times, spreading and transmission loss, and source and receiver impedance coupling terms. Not shown in (1) is a term for anelastic absorption due to Q. A practical approach is adopted, with values per layer per ray type (qP, qSv, Sh) rather than a full anisotropic Q treatment; the ray tracer returns the average Q for each ray. A Futterman-type absorption-dispersion model is used. While the sum over rays may include mode conversions, reflections and head waves in a future version, presently only the three direct arrival types are considered in the data model.

We construct a general moment tensor source using an approach valid in general anisotropic media that may include an explosion (implosion), opening (closing) and slip, an "EOS" source. The O and S parts come from the model of a displacement discontinuity (*DD*) across a plane (e.g. Aki and Richards, 2002), given fracture plane unit normal $\hat{\mathbf{n}}$ and unit displacement direction $\hat{\mathbf{d}}$. The general moment tensor source may then be written (Chapman and Leaney, 2011):

$$\mathbf{M} = \mathbf{M}_{EXP} + \mathbf{M}_{DD} = \kappa[V]\mathbf{I} + \mathbf{c}:A[d](\hat{\mathbf{d}}\,\hat{\mathbf{n}}^T + \hat{\mathbf{n}}\,\hat{\mathbf{d}}^T)/2, \tag{2}$$

where κ is the effective anisotropic modulus, *[V]* is the change in volume due to a change in hydrostatic pressure, $\mathbf{c}$ is the stiffness tensor at the source, *A* is the area of the fracture and *[d]* is the total displacement across the fracture. Two angles specify the fracture normal direction; the displacement vector requires two more angles. Those may be specified by a rake angle of slip in the fracture plane and the angle that $\hat{\mathbf{d}}$ makes with $\hat{\mathbf{n}}$.

We seek to invert (1) for $\mathbf{M}(\omega)$ using a calibrated, layered VTI model and recorded microseismic data transformed to the frequency domain. Equation (1) may be written in matrix-vector form $\mathbf{d}=\mathbf{Gm}$ and solved for $\mathbf{m}$ at each frequency independently, producing a vector of six complex numbers each containing an unknown source function. Inversion for all six elements of the moment tensor requires sufficient sampling of the focal sphere (e.g. Eaton, 2009), which, considering deep borehole monitoring, generally translates to needing downhole receiver arrays in at least two wells. The moment source inversion makes use of a complex SVD routine, matrix scaling or preconditioning, iterative reweighting by residuals for robustness and a regularization parameter estimated using generalized cross validation. Since the matrix inversion process effectively reverses the sign multiplying time and undoes losses due to propagation, the inversion

procedure is called "least-squares time reversal" or simple "*LTRev*" (Leaney, 2008) and can be viewed as a type of vector beam forming. Given the vector beam-formed estimates of the moment tensor elements at each frequency, complex principal components analysis is used to estimate the common source function or wavelet. A weighted, regularized deconvolution step then returns the scaled, real moment tensor elements. Since the input data may be in units of particle velocity or acceleration, the estimated source function is converted to displacement and its amplitude spectrum further analyzed with a 3-term fit to extract the low frequency scalar moment and corner frequency. For the nonlinear problems of event location and model calibration, an objective function is constructed using the inverted moment sources and the forward model (1) to reconstruct the input data and compute the waveform misfit.

Given the estimated moment tensor we seek to recover the EOS representation of the source. To do this a new decomposition is used (Chapman and Leaney, 2011). In the new decomposition a search is first done to determine the isotropic part M_{EXP} which when subtracted from M will, after multiplication by the compliance tensor of the source medium (Vavrycuk, 2005), produce a potency tensor with zero intermediate eigenvalue. This is a unique characteristic of a *DD* source. Such a potency source tensor may be decomposed in terms of its size (area times displacement) and angles: two each for fault normal and displacement vectors or equivalently two for fault normal, one for slip (rake) and one for the angle between the displacement vector and fault normal. Ambiguities remain between fault normal and displacement vectors. We call the decomposition of the *DD* part of the moment tensor into Opening and Slip components the potency tensor bi-axes decomposition. The relative size of the purely isotropic part is determined by dividing M_{EXP} by the effective anisotropic modulus, κ. Together they comprise the new EOS source decomposition. Importantly, the EOS components come in units of volume and can be displayed in true relative size, although for the purpose of comparison in the following section, they are normalized.
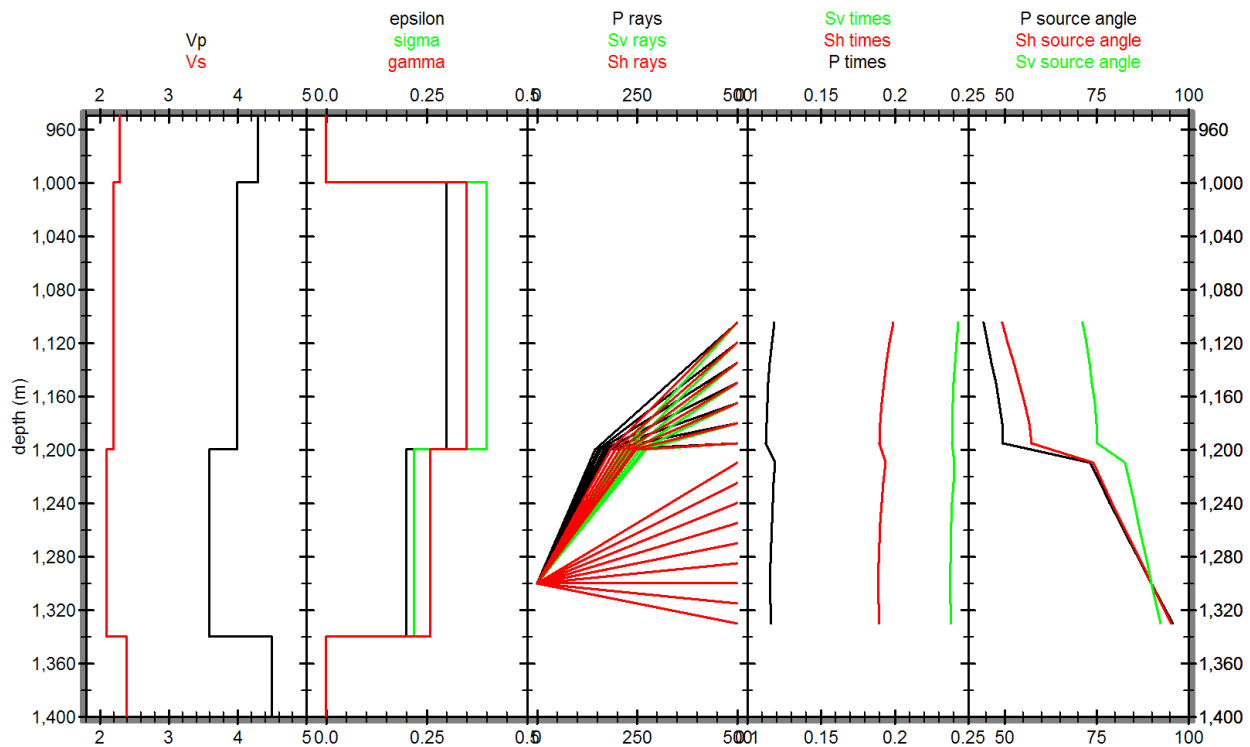

Figure 1. qP (black), qSv (green) and Sh (red) rays from a source location to 16 receivers with the layered VTI model used for the synthetic test. Also shown are times and source take-off angles.

Synthetic example

To demonstrate features of the above inversion procedure 21 microseismic events are simulated with additive noise using equation (1) and the geometry from a real HFM survey. The survey utilized two 8-level receiver arrays in slightly deviated monitoring wells. The velocity model used for simulation is typical of many North American shale gas plays, with an anisotropic shale bounded by faster isotropic carbonates. Anisotropy parameters in the upper shale are: $\varepsilon=0.30$, $\sigma=(V_p/V_s)^2(\varepsilon-\delta)=0.40$, $\gamma=0.35$. Figure 1 shows qP, qSv and Sh rays from an event in the shale to an array of 16 receivers with a spacing of 15m. Also shown are times and source take-off angles as measured from vertical up. The depth of the base of the shale was set so that some of the events would be located in the isotropic carbonate layer below. For the synthetic source pulse, a minimum phase far-field displacement signal is used with spectrum $S(f)=M_0/[(1+(f/f_c)^n]$; $\eta=2$ (Aki and Richards, 2002, eq. 10.38) and corner frequency $f_c =150$Hz. For the source mechanism, we chose a pure slip with oblique relative motion as a special case of a general source. Parameters used were $A[d]=1$ and (strike,dip,rake)= (20,40,60) for all events.
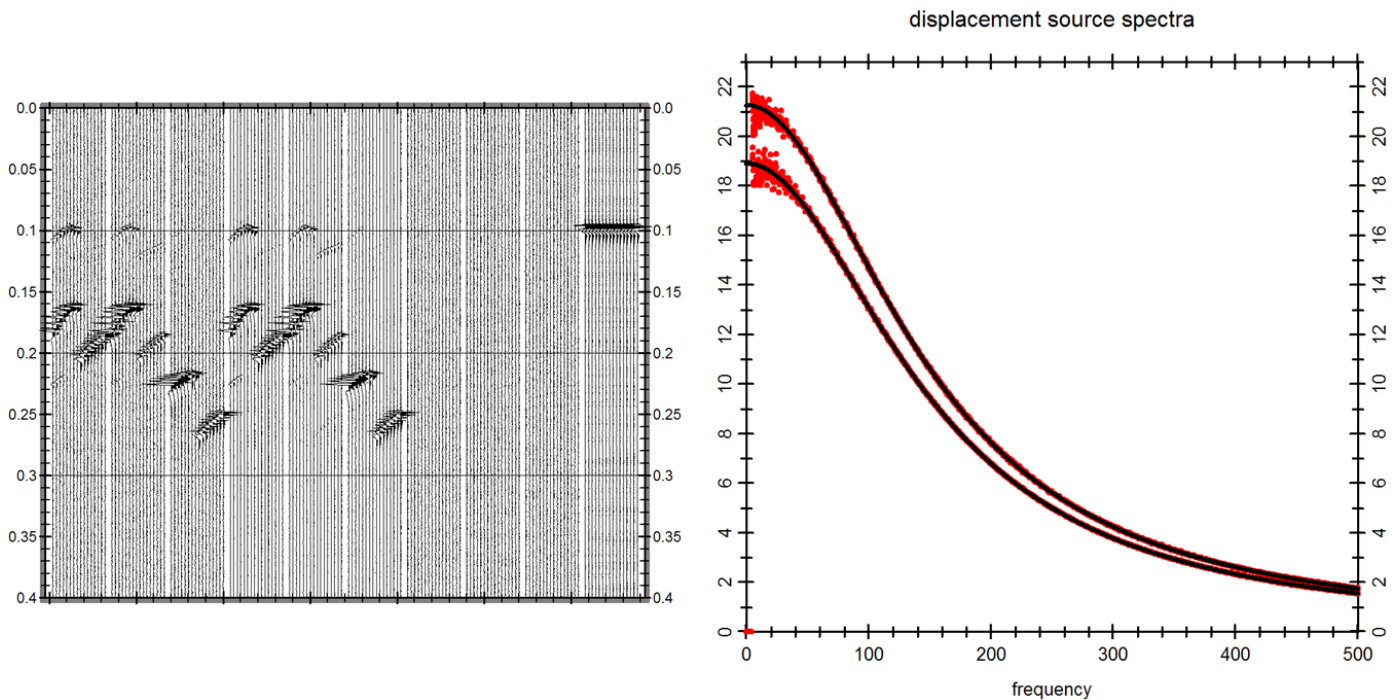

Figure 2. Left: LTRev (Least-squares Time Reversal) waveform QC display for a single event. From left to right: the input East, North, Up (ENU) components for the dual well synthetic; reconstructed ENU data using the estimated source function and forward model; residual ENU data and estimated source pulse shifted to the time of the first P arrival and repeated. Right: Source function displacement spectra for all 21 events with 3-term fit ($M_0, f_c \eta$).

Figure 2 shows the results of the least-squares time reversal waveform inversion. Shown are the input ENU (East,North,Up) data, the reconstructed ENU data, residual ENU data and estimated source function shifted in time to the first P arrival. The source function is shown normalized and repeated for display. Figure 2 also shows the source function transformed to displacement along with a three term fit to determine ($M_0, f_c \eta$). M_0, the scalar moment, is the zero frequency intercept. Two curves are present since the scalar moment differs between the shale and the stiffer carbonate.
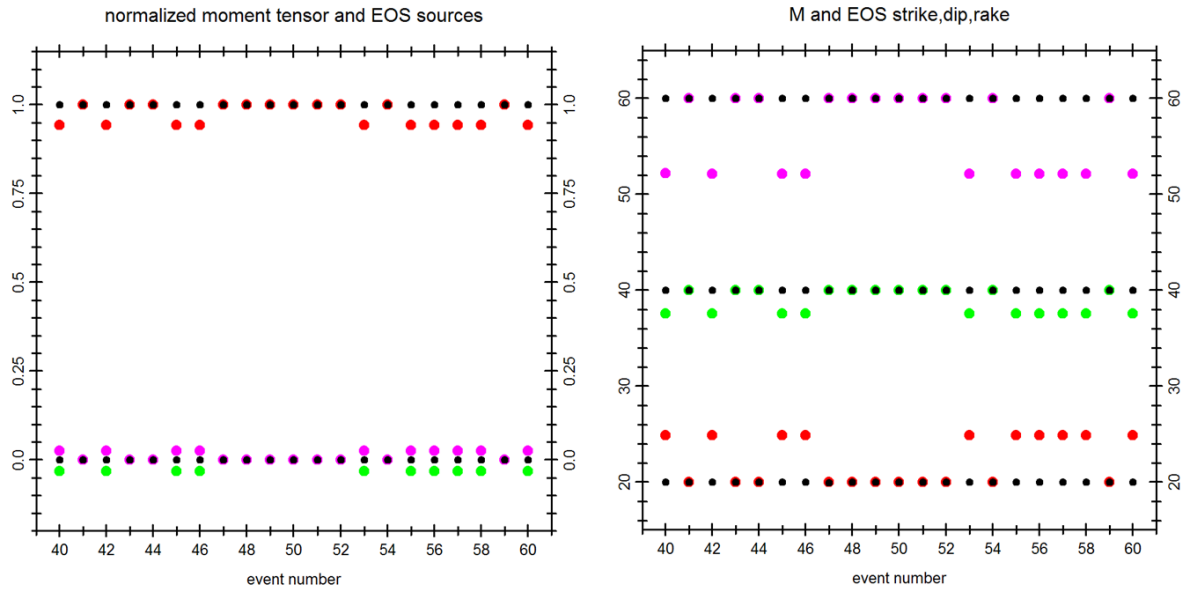
Figure 3. Moment tensor decomposition results versus event number for 21 sources. Left: The traditional normalized basic sources (DC=red, CLVD=green, ISO=magenta) and the new EOS components (black). Events in the anisotropic layer exhibit false non-DC components while the EOS components correctly identify the pure slip mechanism. Right: Focal plane solutions from the moment tensor and from the slip vector obtained from the EOS decomposition. Strike=red, dip=green, rake=magenta. In the anisotropic layer the angles are in error from the traditional moment tensor but correctly recovered with EOS.

Moment tensor decomposition results are shown for the 21 events in Figure 3, plotted versus event number. The results are shown in two ways, as normalized source proportions and slip angles. Looking at the normalized basic sources (M_{iso}, M_{clvd}, M_{dc}) and EOS components, note the bimodal distribution to the basic sources. This is because roughly half of the events were located in the anisotropic shale layer, and the non-vertical displacement in the source causes non-DC components, even though the source mechanism contains only slip. The EOS decomposition, as it de-factors the medium from the moment tensor, correctly identifies all sources as having only an S or slip component. Figure 3 also shows strike, dip and rake angles determined from the moment tensor and from the potency tensor. Solution ambiguity was resolved by selecting from the dual solutions according to the fault normal vector closest to a prior direction (taken as the true fault normal direction). Again we see the impact of anisotropy and the success of the EOS decomposition; angles are rotated significantly from a traditional moment tensor focal plane solution (rake is off by 8 degrees) but angles are correctly recovered with EOS.

Conclusions

The anisotropy of sedimentary rocks is an important property to include in microseismic forward and inverse schemes. We have incorporated VTI anisotropy rigorously in a ray theory – based waveform inversion for a complete moment tensor and source function. The inversion operates in the frequency domain, effectively reversing time by back propagating vector data to the source location, after which source function estimation and deconvolution yield the moment tensor. A new decomposition is then applied to the moment tensor, removing the effect of the anisotropy local to the source and allowing the EOS (Explosion, Opening and Slip) components to be obtained. Our hope is that these new analysis tools will spawn new interpretation strategies to better understand the hydraulic fracturing process.

References

Aki, K. and Richards, P.G., 2002, *Quantitative Seismology*, Second Edition, University Science Books.

Chapman, C.H., 2004, *Fundamentals of Seismic Wave Propagation*, Cambridge University Press.

Chapman, C.H. and Leaney, W.S., 2011, A new moment tensor decomposition for microseismic events in anisotropic media: theory, *Geophys. Journal International*, in preparation.

Eaton, D.W., 2010, Resolution of microseismic moment tensors, SEG Expanded Abstracts, **28**, 2789-2793.

Leaney, W.S. and Chapman, C.H., 2010, Microseismic sources in anisotropic media, 72nd EAGE Extended Abstracts.

Leaney, W.S., 2008, Inversion of microseismic data by least-squares time reversal and waveform fitting, SEG Expanded Abstracts, **27**, 1347-1351.

Vavryčuk, V., 2005, Focal mechanisms in anisotropic media, *Geophys. J. Int.*, **161**, 334-346.